

# Noise Invariant Convolution Neural Network for Segmentation of Multiple Sclerosis Lesions from Brain Magnetic Resonance Imaging

<https://doi.org/10.3991/ijoe.v18i13.34273>

Swetha M D<sup>1,2</sup>(✉), Aditya C R<sup>2</sup>

<sup>1</sup>B.M.S. College of Engineering, Bengaluru, India

<sup>2</sup>Vidyavardhaka College of Engineering, Mysuru, India

shwetha9918@gmail.com

**Abstract**—The objective of the research work is to accurately segment multiple sclerosis (MS) lesions in brain Magnetic Resonance Imaging (MRI) of varying sizes and also to classify its types. Designing effective automatic segmentation and classification tool aid the doctors in better understanding MS lesion progressions. In meeting research challenges, this paper presents Noise Invariant Convolution Neural Network (NICNN). The NICNN model is efficient in the detection and segmentation of MS lesions of varying sizes in comparison with standard CNN-based segmentation methods. Further, this paper introduced a new cross-validation scheme to address the class imbalance issue by selecting effective features for classifying the type of MS lesion. The experiment outcome shows the proposed method provides improved Dice Similarity Coefficient (DSC), Positive Predicted Value (PPV), and True Positive Rate (TPR) value compared to the state-of-art CNN-based MS lesion segmentation method. Further, achieves better accuracy in classifying MS lesion types compared to standard MS lesion type classification models.

**Keywords**—convolution neural network classification, deep learning, denoising, magnetic resonance imaging, multiple sclerosis, segmentation

## 1 Introduction

Multiple Sclerosis is one of the most predominant neurological diseases, where MRI scans, are usually used for its diagnosis. However, better detection and monitoring of multiple sclerosis is an urgent need [1]. Especially, segmentation of new lesions at an early stage is of utmost importance. In segmentation of new lesion prerequisite: a) MRI scans of the same patient with different time points and b) radiologists by studying the MRI scan of different points can identify new lesion. The prerequisite induces two issues [2] such as they are prone to provide a segmentation error and it is extremely time-consuming considering the size and multi-dimensionality nature of data. Alongside, MRI scan provides images with different contrast levels making segmentation an extremely challenging task as shown in Figure 1.

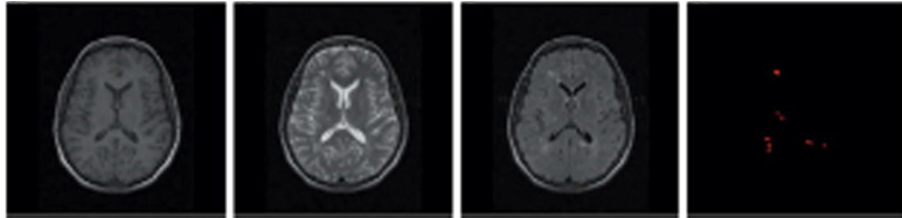


**Fig. 1.** A slice of a brain MRI scan with the presence of MS lesions: T1-w, T2-w, and FLAIR, from left to right, respectively

Deep learning (DL) methods have proven useful for the segmentation of MS lesions in brain MRI scans [3]. However, the existing method exhibits poor segmentation outcomes considering both small and large lesions together [4]. Further, the presence of motion artifacts in training image impact segmentation performance. Further, the existing method fails to establish correlation considering different lesion types by the different radiologists as shown in Figure 2 and when out-of-distribution generalization and data is an imbalance in nature, the model exhibits poor classification accuracies [5, 6].

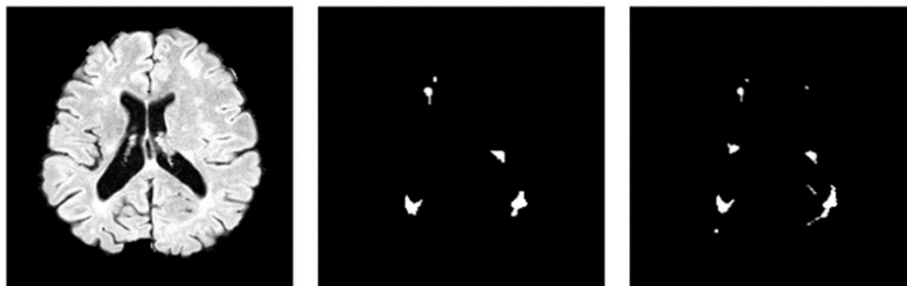


**Fig. 2.** Brain MRI scan with biomarker mask from two radiologists: MRI, Biomarker mask by radiologist 1, Biomarker mask by radiologist 2, from left to right, respectively

This paper presents noise invariant CNN for the segmentation of new lesions from brain MRI scans. Further, design a new cross-validation scheme that addresses class imbalance issues through effective feature optimization for MS lesion type classification.

### 1.1 The significance of the research work is given below

The proposed model achieves higher DSC, PPV, and TPR than the exist-ing CNN-based segmentation model; thus, is very efficient in segmenting both small and large MS lesions. The model introduced a new feature selection optimization method through an improved cross-validation method for solving multi-label classification under imbalanced data. The classification model achieves higher accuracies for MS lesion-type classifications in comparison to standard models.

## 2 Literature survey

This section surveys various recent brain MS lesions, and segmentation models. In [5], focused on designing robust and fast automatic segmentation of white matter hyperintensities concerning age-factor and also MS lesion from 3D T2-FLAIR and 3D T1-weighted datasets. Their model depends on the merging of watershed parcellation and non-linear diffusion structure for selection of intensity and location pattern and refinement of segmentation is done. In [6] aimed at designing a simple and robust supervised cluster-based MS lesion segmentation model for carrying out a quantitative study using MRI scans of different types such as FLAIR, T1-weighted, and T2-weighted. The clustering method used the Euclidean distance function for classification operation. In [7] focused to design a model for estimating relaxation parameter maps to distinguish white matter from normal-appearing brain tissues. The spatial normalized the MRI using the pipeline method by fitting multivariate polynomial regression. In [8] focused on segmenting MS lesions by studying lesion dimensions and grayscale features. A cellular learning automaton is designed using reward and penalty through a trial-error mechanism for each pixel.

In [9] designed three-dimensional CNN for automatic segmentation of MS lesions from brain MRI scans. The three-dimensional CNN encompasses two convolution and two pooling layers. Initially, the substitute lesion voxels are chosen, then the eventual lesion voxels are segmented from the initially obtained lesions using certain constraints. In [10] the deep gray matter and white matter lesions are segmented for quantification of MS in brain MRI scans using CNN [11]. The model provided reliable and fast segmentation of gray matter and MS lesion using multi-model MRI scans.

In [12], a new CNN is introduced for the segmentation of MS lesions using brain MRI scans. They used a filter size of  $3 \times 3$  or  $5 \times 5$  for segmenting MS lesions of different sizes. However, selecting of using which filter is very difficult. In addressing the issues, they introduced the inception module into Google Net. The inception module in a parallel manner uses  $3 \times 3$ ,  $5 \times 5$ ,  $1 \times 1$ , and max pooling filters. The improvised model achieves a better MS lesion segmentation outcome than the standard CNN model [32, 33]. In [28] showed that the UNET architecture are very good in performing segmentation of tumor in Kidney using CT images. However, tumor segmentation using brain MRI [29] is challenging due to presence of motion artifacts; thus, requires efficient preprocessing technique [30, 31]. In [13] the UNET framework is modified by using the wavelet transformation function in the pooling layer rather than the max pooling function. The model is effective in detecting edge and local features more efficiently with the limited number of features. When applying the transformation, it exhibits a multi-resolution pattern; thus, enhancing segmentation outcomes with varying lesion sizes. In [14], designed an MS lesion segmentation framework using T2 and FLAIR MRI scans. They modified the attention UNET (MAUNET) and also modified the UNET (MUNET) by introducing additional preprocessing and loss functions [15]. the model attains better performance than standard UNET [16] and attention UNET. In [17] showed how the ensemble model how ensemble is efficient in detecting and segmentation of different MS lesion types. However, the standard cross-validation scheme

used exhibits very poor performance when data is imbalanced in nature [18, 19]. In addressing the research challenges in the next section an improved segmentation and lesion type classification model is presented.

### 3 Proposed methodology

In this work, Noise Invariant CNNs (NICNNs) is designed for the segmentation of MS lesion segmentation from brain MRI. In this work, first, the standard UNET architecture is described, followed by an introduction of additional noise invariant layer into UNET to obtain NICNNs. Later, an edge-preserving sparse view frame is designed for feature learning, also in achieving higher learning rate efficiency the batch normalization operation is optimized. Finally, an improved feature optimization model is introduced to address the class imbalance issue for MS lesion type classifications.

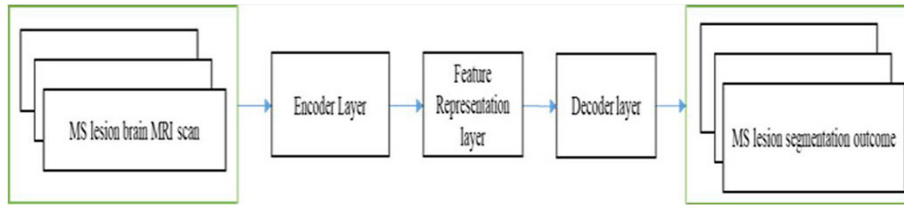


Fig. 3. Standard CNN encoder-decoder framework

#### 3.1 Optimization of convolution neural network

The UNET architecture also emphasizes a similar structure as CNN shown in Figure 3 with multiple convolutions in every layer. Alongside, the activation function plays a comparable part for the presented filter after kernel coefficients, resulting in non-linear behavior. The outcome results in a fully connected convolution neural network as defined below

$$a^g = \{a_1^g, a_2^g, \dots, a_{I_g}^g\} \quad (1)$$

convolution with the kernel is expressed as follows

$$u^g = \{u_1^g, u_2^g, \dots, u_{I_g}^g\} \quad (2)$$

bias parameter is obtained as follows

$$z^g = \{z_1^g, z_2^g, \dots, z_{I_g}^g\} \quad (3)$$

and activation of the  $i^{th}$  layer is computed as follows

$$a_h^g = f(u_h^g \otimes B(a^{g-1}) + z_h^g) \in a^g, 1 \leq g \leq I_g, \quad (4)$$

$$a^g \equiv A^g(B(a^{g-1}); \tau^g), 1 \leq g \leq j, \quad (5)$$

where  $f(\cdot)$  defines activation function,  $\otimes$  defines a convolutional function,  $B(\cdot)$  defines the pooling function of  $(\cdot)$ , and  $\tau^g$  defines the complete parameter used in the  $i^{th}$  layer. The adoption of the pooling function aid in reducing the number of parameters used in generating global features of brain MS lesions. The rectifier linear unit (RELU) provides better performance than sigmoid function; thus, in this work parameterized RELU is used for better learning of small features of brain MS lesions through parametrized optimization of biases and weight. The mathematical representation of the feed-forward activation function is described as follows

$$f(v) = \begin{cases} v & \text{if } v > 0 \\ (\omega)v & \text{if } v \leq 0 \end{cases} \quad (6)$$

The modified parameterized RELU is defined as follows

$$f(v) \equiv \max(v, 0) + (\omega) \min(0, w) \quad (7)$$

The value of  $\omega$  is set in a range between 0 to 1 and the outcome of the feed-forward network is obtained as follows

$$(G; \tau) = \tilde{A}^{2j-1} \left( \begin{array}{c} \dots \tilde{A}^{j+1} (A^j (\dots A^2 (G; \tau^1); \tau^2) \dots; \tau^k); \\ (\tau^{k+1}) \dots; \tau^{2k-1} \end{array} \right) \quad (8)$$

where  $G$  defines the input that is similar to the pooling of Eq. (4) and (5) and  $\tau$  is defined as follows

$$\tau = \{\tau^1, \tau^2, \dots, \tau^{2j-1}\} \quad (9)$$

The outcome of the convolutional layer is defined in below equation

$$\dot{a}^q = \tilde{A}^q(S(\dot{a}^{p-1}); \delta^p), j+1 \leq p \leq 2j-1 \quad (10)$$

$$\dot{a}_r^q = e(u_o^p \otimes S(\dot{a}^{p-1}) + z_o^p) \in \dot{a}^q, 1 \leq o \leq L_p, \quad (11)$$

where  $\dot{a}^q$  defines the bias parameter of layer  $p$ ,  $\tilde{A}^q$  defines convolution layer outcome of matrix reconstruction,  $S(\cdot)$  defines upsampling for reconstructing the original matrix. The convolution kernel for the decoding process is obtained as follows

$$u^p = \left\{ u_1^p, u_2^p, \dots, \dots, u_{L_p}^p \right\}, \quad (12)$$

and bias outcome of decoding operation of  $p^{th}$  layer is given as follows

$$z^p = \{z_1^p, z_2^p, z_{L_p}^p\}, \quad (13)$$

The parameter  $\delta$  is updated through the backpropagation process iteratively according to gradient descent for minimizing the predefined loss as follows

$$\operatorname{argmin}_{\tau} E(A(G; \tau); M) \quad (14)$$

where  $E$  defines loss operation and  $M$  defines the expected outcome.

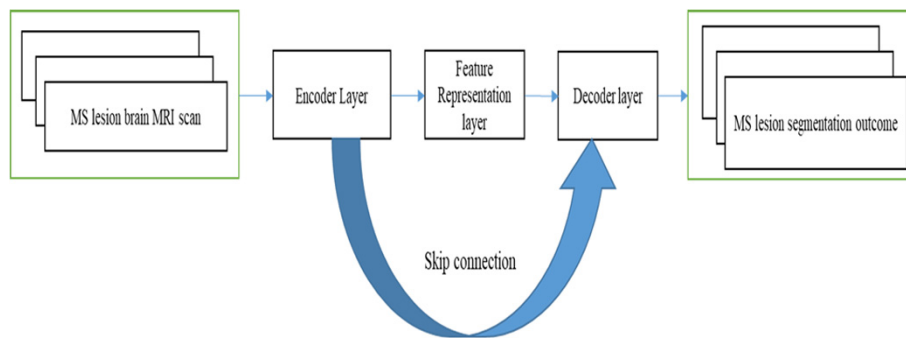


Fig. 4. The proposed noise invariant CNN framework

### 3.2 Noise invariant convolution neural network

In this section, a noise invariant convolution neural network is introduced as shown in Figure 4. The NICNN is iteratively applied to extract features from low-resolution MS lesion brain MRI. The NICNN with noise invariant skip connection is expressed as follows

$$A = \mu^{trans} F_{\omega}(d)\varphi \quad (15)$$

where  $\mu^{trans}$  defines the pooling function,  $F_{\omega}$  defines the catalecticant matrix for obtaining convolution and  $\varphi$  defines the lowpass filter. The above equation is used for obtaining a sparse coefficient of convolution. The CNN autoencoder with skip is expressed through the following equation

$$W = \begin{bmatrix} A \\ Q \end{bmatrix} = Y(d \otimes \varphi) \quad (16)$$

where the parameter used in the above equation is expressed below

$$Y = \begin{bmatrix} I - M \\ \mu^{trans} \end{bmatrix} \quad (17)$$

where  $I - M$  represent the identity matrix,  $Y$  defines extended pooling of NICNN,  $A$  defines the bypass component and obtained as follows

$$A = (d \otimes \varphi) \quad (18)$$

and  $Q$  defines the low pass band and obtained as follows

$$Q = \mu^{trans} (d \otimes \varphi) \quad (19)$$

where  $(d \otimes \varphi)$  define multi-channel convolution in CNN.

### 3.3 Improved feature learning

The noise invariant CNN introduces an improved feature learning by modeling the edge-preserving sparse view frame; from the above equation edge-preserving sparse view frame is expressed in the following equation

$$\ddot{Y} = \frac{1}{(I - M + \mu^{trans}\mu)} [I - M\mu] \quad (20)$$

The matrix inversion for average sensitivity edge-preserving sparse view frame CNN is obtained in the below equation

$$\ddot{Y} = \left[ I - \frac{\mu^{trans}\mu}{2} \left( \frac{\mu}{2} \right) \right] \quad (21)$$

Using sparse coefficient  $W$ , the segmentation network model of NICNN is given below

$$\dot{A} = A + S(Q - \mu^{trans}A) \quad (22)$$

where  $S$  defines unpooling and  $(Q - \mu^{trans}A)$  defines residual.

### 3.4 Segmentation using optimized feature and learning

The segmentation of MS lesion in brain MRI exhibit poor accuracies in the edge region. Then, UNET-based segmentation methods exhibit higher redundant features and fail to establish global features for high-resolution input MS lesion brain MRI  $d^{k+1}$ . The parameter  $d^{k+1}$  defines the redundant features. The problem definition without the presence of convolution on the respective layer is given as follows

$$n^{j+1} = a^{j-1} \oplus S(\vartheta^k) \quad (23)$$

where  $\oplus$  combines two MS lesion brain MRIs before and after applying the operator. In NICNN, the remaining path is used for neglecting redundant features in the local feature map. The remaining path is provided immediately after pooling. Therefore, a global feature map can be passed through skip connections, and in optimizing the filter performance a parameter  $\mathcal{P}$  is defined. The feature map before and after the path is considered. If  $FM_2(v,w) < 0.01$  then,

$$\mathcal{P} = -0.5 \quad (24)$$

Otherwise,

$$\mathcal{P} = \frac{\sum_{v,w \in \text{object}} \text{label}(v,w) FM_z(v,w)}{\sum_{v,w \in \text{object}} \text{label}(w,z) FM_z(v,w)} \quad (25)$$

After obtaining the optimized features, the learning rate is optimized by minimizing complexity through batch normalization. In this work, batch normalization first subtracts the mean and the divides using standard deviation. Thus, aiding in achieving a better convergence rate with fewer dependencies on input distribution. This work considers layer with  $c$  – dimensional input  $V = (v^{(1)} \dots v^{(c)})$  and establishes the normalization of each dimension as follows

$$\hat{v}^{(i)} = (v^{(i)} - C[v^{(i)}])(Var[v^{(i)}])^{-1/2} \quad (26)$$

Then, the batch  $Z$  of size  $k$  and normalization is performed on every activation self-reliantly as follows

$$Z = \{v_{1, \dots, k}\} \quad (27)$$

The normalized outcome provides a linear transformation as follows

$$batch_{norm}: v_{1, \dots, k} \rightarrow w_{1, \dots, k} \quad (28)$$

The outcome of the above equation is added to the network for achieving a higher learning rate aiding segmentation accuracies of MS lesions of varying sizes.

### 3.5 Feature selection optimization for MS lesion type classification

In [20, 21, 22] focused on detecting different MS lesion types using segmentation biomarkers of brain MRI. The aforementioned models train the classification models by building a regression tree using the following  $K$ -fold cross-validation scheme

$$CV(\sigma) = \frac{1}{M} \sum_{k=1}^K \sum_{j \in G_{-k}} P(b_j, \hat{g}_{\sigma}^{-k(j)}(y_j, \sigma)) \quad (29)$$

Using the above equation, the standard model first divides the MS lesion type classification dataset into  $a$   $K$  subset of identical size in a random manner. Then  $K - 1$  subset is used for designing the MS lesion type classification model and reaming subset is used for minimizing prediction error. However, when data is imbalanced these models exhibit very poor MS lesion type classification outcomes, as they fail to establish the correlation among features (i.e., biomarkers) concerning different types of MS lesions.

In this work, a multi-level cross-validation scheme is introduced for establishing a correlation among features. In the first level, feature subsets are selected as important features. In the second level, the main subset feature chosen from the first level is used for constructing a new cross-validation method as follows

$$CV(\sigma) = \frac{1}{SM} \sum_{s=1}^S \sum_{k=1}^K \sum_{j \in G_k} P(b_j, \hat{g}_\sigma^{-k(j)}(y_j, \sigma)) \quad (30)$$

In equations (30),  $M$  defines the size of training data used,  $P(\cdot)$  defines the loss function, and  $\hat{g}_\sigma^{-k(j)}(\cdot)$  defines a function for estimating coefficients. Then, the feature optimization in choosing ideal  $\hat{\sigma}$  is computed as follows

$$\hat{\sigma} = \arg \min_{\sigma \in \{\sigma_1, \dots, \sigma_j\}} CV_s(\sigma) \quad (31)$$

By solving the above optimization constraint, the MS lesion type classification accuracies are improved.

## 4 Results and discussion

This section provides the segmentation efficiency of the proposed NICNN over the existing UNET-based model [12, 14, 27]. The proposed model is implemented using Python 3 and MATLAB framework using Windows 10 operating system running on I-7 quad-core processor, with 16GB RAM and CUDA-enabled 4GB GPU. The MS lesion brain MRI is collected from [23, 24] ISBI 2015 challenge dataset which provides similar data in [25, 26]. The dataset has 19 patients' MRI scans of T1-weighted, T2-weighted, and FLAIR., out of which 5 MRIs annotated by two physicians are used for training, and the remaining MRIs are used for validating models. More details of the dataset used can be obtained from [25, 26]. The metric used for experiment analysis is DSC, PPV, and TPR.

The DSC similarity defines a measure of similarity among segmented outcome with respect to its ground truth. Higher value defines better segmentation performance. The DSC is computed as follows

$$DSC = \frac{2TP}{2TP + FP + FN} \quad (32)$$

The PPV indicates proportion of true positive lesions extracted during automatic segmentation. Higher value defines better segmentation performance. The PPV is computed as follows

$$PPV = \frac{TP_{AS}}{N} \quad (33)$$

where  $TP_{AS}$  defines the number of lesions correctly classified using ground truth with respect to number of lesions in automatic segmentation and  $P$  defines the number of lesions in automatic segmentation.

The true positive rate defines proportion of the detected lesions in the ground truth. Higher value defines better segmentation performance. The TPR is computed as follows

$$TPR = \frac{TP_{GT}}{Q} \quad (34)$$

where  $TP_{GT}$  defines the number of lesions correctly classified using automatic segmentation with respect to ground truth and  $Q$  defines the number of lesions in automatic segmentation.

#### 4.1 Segmentation outcome

This section provides the architecture configuration of NICNN as shown in Table 1 and graphical representation of segmentation outcome of proposed NICNN over existing segmentation model namely MUNET [14] and MAUNET [14]. The layer size, parameter size, training and testing time is shown in Table 1. From Table 2 we can see that the NICNN uses a lesser number of layers in comparison with MUNET [14]; further, NICNN reduces the training time using sparse-based feature extraction; thus, reduces number of features extracted and aiding in reduction of training time; further, the the NICNN reduces testing time i.e., it reduces time to perform segmentation in comparison with MUNET.

**Table 1.** Architecture of NICNN

Layer Name	Kernel Size	Number of Filter	Activation
conv	3*3	64	relu
conv	3*3	64	relu
maxpool	2*2	–	maxpool
tconv	3*3	64	relu
conv	3*3	64	relu
deconv	2*2	–	–
conv	3*3	64	relu
conv	3*3	64	relu
conv	3*3	128	relu
conv	3*3	128	relu
maxpool	2*2	–	maxpool
tconv	3*3	128	relu
conv	3*3	128	relu
deconv	2*2	–	–
conv	3*3	128	relu
conv	3*3	128	relu
conv	3*3	256	relu
conv	3*3	256	relu
maxpool	2*2	–	maxpool
tconv	3*3	256	relu
conv	3*3	256	relu
deconv	2*2	–	–
conv	3*3	256	relu
conv	3*3	256	relu
conv	3*3	512	relu
conv	3*3	512	relu
maxpool	2*2	–	maxpool
tconv	3*3	512	relu
conv	3*3	512	relu
deconv	2*2	–	–
conv	3*3	512	relu
conv	3*3	512	relu
conv	3*3	1024	relu
conv	3*3	1024	relu
conv	1*1	1	relu

The segmentation outcome of proposed with respect existing MUNET [14] is shown in Figure 5. Similarly, the segmentation outcome of proposed with respect existing MAUNET [14] is shown in Figure 6. From the result obtained it can be seen the NICNN achieves very good segmentation outcome in comparison with existing segmentation methodologies.

**Table 2.** Layers, parameter, training, and testing time

Methodology	Number of Layers	Number of Parameters	Training Time (Seconds)	Evaluation Second
MUNET [14]	41	1941101	9800	8.45
NICNN	30	1786690	6800	5.15

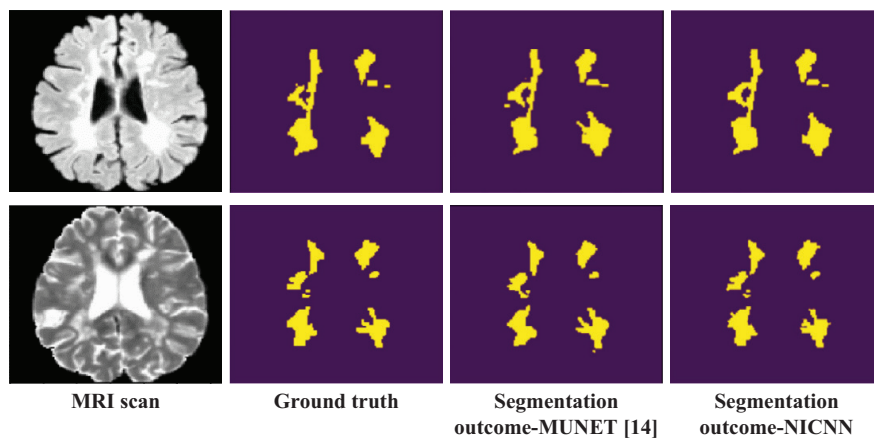


**Fig. 5.** MRI scan used for validating proposed NICNN over existing Modified UNET, 2022

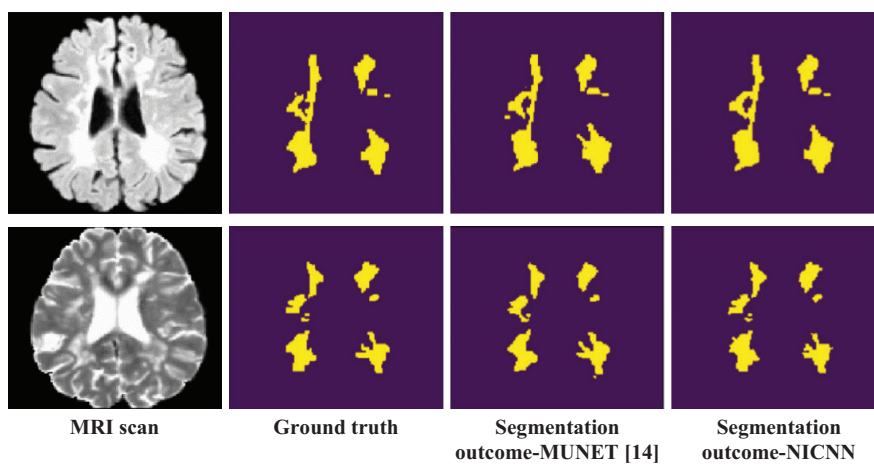


**Fig. 6.** MRI scan used for validating proposed NICNN over existing Modified Attention UNET, 2022

#### 4.2 MS lesions segmentation performance analysis

The section provides the performance efficiency of the proposed NICNN-based MS lesion segmentation outcome in comparison with existing CNN-based segmentation models such as Attention UNET (AUNET, 2020) [27], CNN binary cross entropy (CNN-BCE, 2021), [12], Modified UNET (MUNET, 2022) [14], and Modified AUNET (MAUNET, 2022) [14].

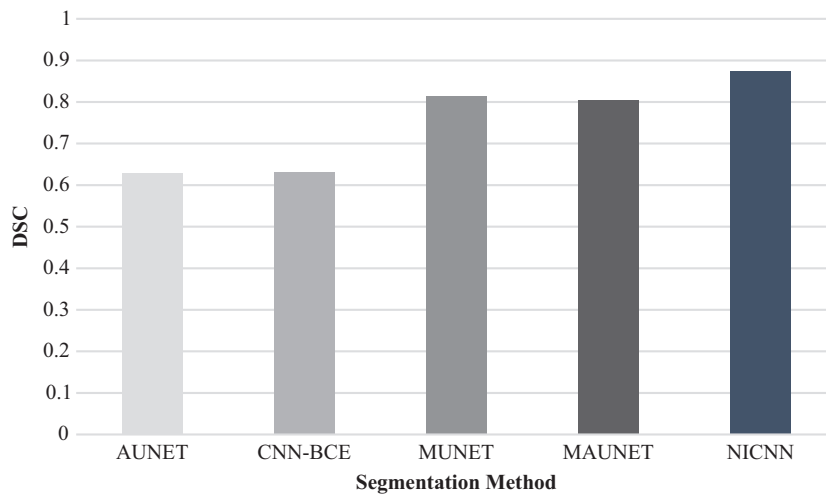


Fig. 7. Dice similarity coefficient

Figure 7 shows a graphical representation of Dice similarity coefficient performance achieved using the proposed NICNN and other existing CNN-based segmentation models. A higher value indicates better DSC performance; thus, the NICNN model achieves better MS lesion segmentation outcome by minimizing false prediction and maximizing classification accuracy in comparison with AUNET, CNN-BCE, MUNET, and MAUNET.

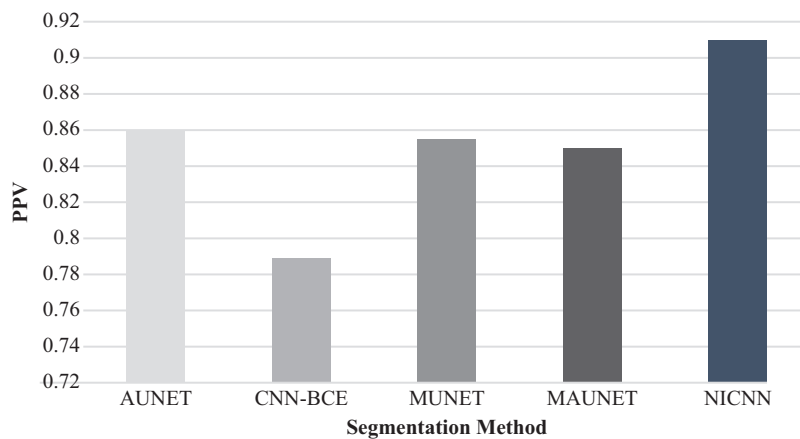
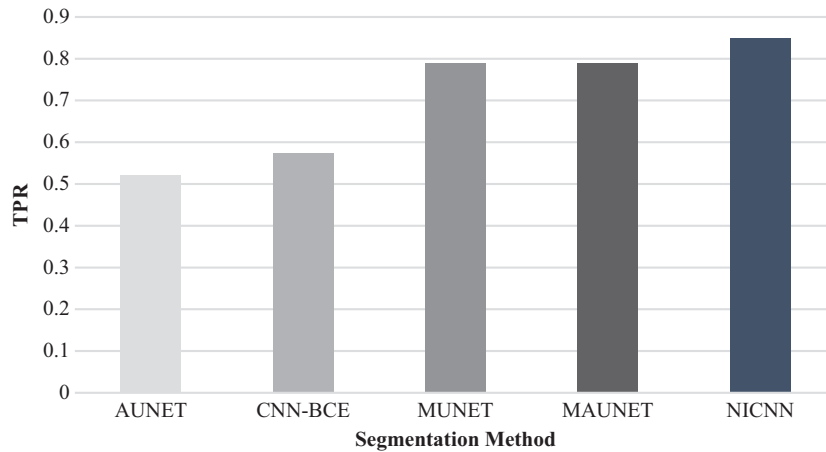


Fig. 8. Positives prediction value



**Fig. 9.** True positives rate

Figure 8 shows a graphical representation of positive prediction value performance achieved using the proposed NICNN and other existing CNN-based segmentation models. A higher value indicates better PPV performance; thus, the NICNN model achieves better MS lesion segmentation outcomes in comparison with AUNET, CNN-BCE, MUNET, and MAUNET. Figure 9 shows a graphical representation of true positive rate performance achieved using the proposed NICNN and other existing CNN-based segmentation models. A higher value indicates better TPR performance; thus, the NICNN model achieves better MS lesion segmentation outcomes by correctly classifying in comparison with AUNET, CNN-BCE, MUNET, and MAUNET.

### 4.3 MS lesions type classification performance analysis

This section provides experiment results using feature selection optimization through an imbalanced data-aware cross-validation mechanism. The proposed feature-aware regression tree (FART) is compared with the regression tree (RT)-based classification [20], [21] model. The classification task is done as a multi-label classification problem. The sub-types are cortex-led, normal-appearing white matter-led, and lesion-led. The graphical representation of the proposed FART and existing RT type classification performance is shown in Figure 10. The result shows the FART achieves much better performance than existing RT methods.

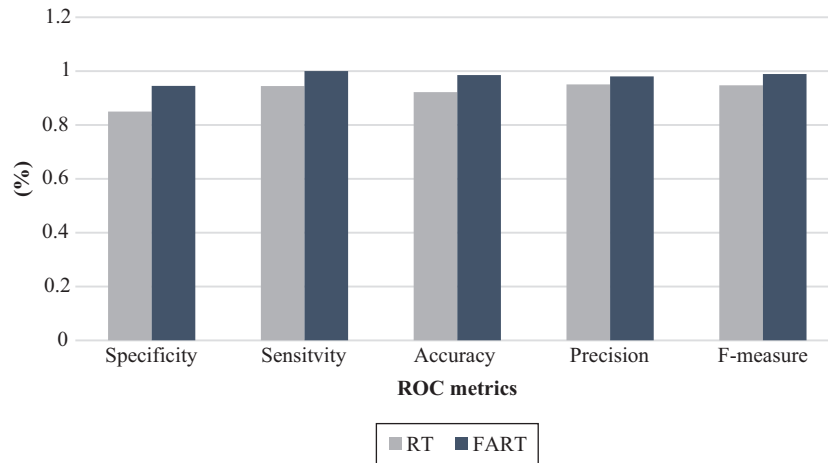


Fig. 10. Classification performance

## 5 Conclusion

The segmentation of MS lesions from brain MRI scans by deep learning methods has enabled the automatic extraction of features from MRI scans and has provided good results compared to traditional image processing methods. In deep learning, U-Net convolutional neural networks are used to segmentation of MS lesions from brain MRI scans. In this network, an improved noise invariant CNN adding a skip connection between encoder and decoder was used to optimize feature extraction considering issues of motion artifact in MRIs. In the proposed method, a pooling layer based on a novel transformation is used for representing sparse coefficient, which has made it possible to highlight the desired features for the extraction of MS lesions in MRI images. This method has high accuracy in detecting and segmentation of lesions of different sizes and has better results than other existing CNN-based segmentation models. Further, a novel feature optimization method is modeled through a modified cross-validation mechanism; aiding in achieving better classification of MS lesions in comparison with a state-of-art model. In future work, the use of more data and 3D implementation is suggested to improve the results.

## 6 References

- [1] Boaventura, M., Sastre-Garriga, J., Garcia-Vidal, A., Vidal-Jordana, A., Quartana, D., Carvajal, R., Auger, C., Alberich, M., Tintoré, M., Rovira, À., Montalban, X. & Pareto, D. T1/T2-weighted ratio in multiple sclerosis: A longitudinal study with clinical associations. *Neuroimage Clin* 34,102967, (2022). Epub 2022 Feb 16. PMID: 35202997; PMCID: PMC8866895. <https://doi.org/10.1016/j.nicl.2022.102967>
- [2] Sah, M. & Direkoglu, C. A survey of deep learning methods for multiple sclerosis identification using brain MRI images. *Neural Comput & Applic* 34, 7349–7373 (2022). <https://doi.org/10.1007/s00521-022-07099-3>

- [3] Kaur, A., Kaur, L. & Singh, A. State-of-the-art segmentation techniques and future directions for multiple sclerosis brain lesions. *Arch Computat Methods Eng* 28, 951–977 (2021). <https://doi.org/10.1007/s11831-020-09403-7>
- [4] Balwant, M.K. A review on convolutional neural networks for brain tumor segmentation: Methods, datasets, libraries, and future directions, *IRBM*, 2022, ISSN 1959-0318. <https://doi.org/10.1016/j.irbm.2022.05.002>
- [5] Philippe Tran, Urielle Thoprakarn, Emmanuelle Gourieux, Clarisse Longo dos Santos, Enrica Cavedo, Nicolas Guizard, François Cotton, Pierre Krolak-Salmon, Christine Delmaire, Damien Heidelberg, Nadya Pyatigorskaya, Sébastien Ströer, Didier Dormont, Jean-Baptiste Martini, & Marie Chupin. Automatic segmentation of white matter hyperintensities: Validation and comparison with state-of-the-art methods on both Multiple Sclerosis and elderly subjects. *NeuroImage: Clinical* 33, 102940 (2022). ISSN 2213-1582. <https://doi.org/10.1016/j.nicl.2022.102940>
- [6] Ozdemir Cetin, Volkan Seymen, & Unal Sakoglu. Multiple sclerosis lesion detection in multimodal MRI using simple clustering-based segmentation and classification. *InformatICS in Medicine Unlocked* 20, 100409 (2020). ISSN 2352-9148. <https://doi.org/10.1016/j.imu.2020.100409>
- [7] Pirozzi, MA., Tranfa, M., Tortora, M., Lanzillo, R., Brescia Morra, V., Brunetti, A., Alfano, B. & Quarantelli M. A polynomial regression-based approach to estimate relaxation rate maps suitable for multiparametric segmentation of clinical brain MRI studies in multiple sclerosis. *Comput Methods Programs Biomed* 223, 106957 (2022). Epub ahead of print. PMID: 35772230. <https://doi.org/10.1016/j.cmpb.2022.106957>
- [8] Moghadasi, M. & Fazekas, Gabor. An automatic multiple sclerosis lesion segmentation approach based on cellular learning automata. *International Journal of Advanced Computer Science and Applications* (2019). <https://doi.org/10.14569/IJACSA.2019.0100726>
- [9] Xiang, Y., et al. Segmentation method of multiple sclerosis lesions based on 3D-CNN networks. *IET Image Process* 14, 1806–1812 (2020). <https://doi.org/10.1049/iet-ipr.2019.0880>
- [10] McKinley, R., Wepfer, R. & Aschwanden, F. et al. Simultaneous lesion and brain segmentation in multiple sclerosis using deep neural networks. *Sci Rep* 11, 1087 (2021). <https://doi.org/10.1038/s41598-020-79925-4>
- [11] Zhang, H. & Oguz, I. Multiple Sclerosis Lesion Segmentation – A Survey of Supervised CNN-Based Methods. In: Crimi, A., Bakas, S. (eds) *Brainlesion: Glioma, Multiple Sclerosis, Stroke and Traumatic Brain Injuries. BrainLes 2020. Lecture Notes in Computer Science* 12658, (2021). Springer, Cham. [https://doi.org/10.1007/978-3-030-72084-1\\_2](https://doi.org/10.1007/978-3-030-72084-1_2)
- [12] Shahab U. Ansari, Kamran Javed, Saeed Mian Qaisar, Rashad Jillani, Usman Haider, “Multiple sclerosis lesion segmentation in brain MRI using inception modules embedded in a convolutional neural network.” *Journal of Healthcare Engineering* 2021, Article ID 4138137, 10 pages, (2021). <https://doi.org/10.1155/2021/4138137>
- [13] Alijamaat, Ali, Alireza Nikravanshalmani & Peyman Bayat. Multiple sclerosis lesion segmentation from brain MRI using U-Net based on wavelet pooling. *International Journal of Computer Assisted Radiology and Surgery* 16, 1459–1467 (2021). <https://doi.org/10.1007/s11548-021-02327-y>
- [14] Hashemi, Maryam & Akhbari, Mahsa & Jutten, Christian. Delve into multiple sclerosis (MS) lesion exploration: A modified attention U-Net for MS lesion segmentation in brain MRI. *Computers in Biology and Medicine* 145, 105402 (2022). <https://doi.org/10.1016/j.combiomed.2022.105402>
- [15] Krüger, J., Ostwaldt, AC. & Spies, L. et al. Infratentorial lesions in multiple sclerosis patients: Intra- and inter-rater variability in comparison to a fully automated segmentation using 3D convolutional neural networks. *Eur Radiol* 32, 2798–2809 (2022). <https://doi.org/10.1007/s00330-021-08329-3>

- [16] Ghodhbbani, G., Sahnoun, M., Kallel F. & Siarry, P. U-NET architecture for automatic MS lesions segmentation using MR images. 2022 6th International Conference on Advanced Technologies for Signal and Image Processing (ATSIP), pp. 1–5, 10.1109/ATSIP55956.2022.9805910, 2022. <https://doi.org/10.1016/j.cmpb.2022.106957>
- [17] Tohidi, Pouria & Remedios, Samuel & Greenman, Danielle & Shao, Muhan & Han, Shuo & Dewey, Blake & Reinhold, Jacob & Chou, Yi-Yu & Pham, Dzung & Prince, Jerry & Carass, Aaron. Multiple sclerosis brain lesion segmentation with different architecture ensembles. 80, (2022). <https://doi.org/10.1117/12.2623302>
- [18] Macar, Uzay & Karthik, Enamundram & Gros, Charley & Lemay, Andreeane & Cohen-Adad, Julien. Team NeuroPoly: Description of the Pipelines for the MICCAI 2021 MS New Lesions Segmentation Challenge, 2021. <https://arxiv.org/abs/2109.05409>
- [19] Nass, M., Mzoughi, H., Njeh, I., Benslimam, M. & BenHamida, A. Computer Aided Diagnosis (CAD) tool for MS lesions exploration In multimodal brain MRI. 2022 6th International Conference on Advanced Technologies for Signal and Image Processing (ATSIP), 2022, pp. 1–6, <https://doi.org/10.1109/ATSIP55956.2022.9805933>
- [20] Eshaghi, A., Young, A.L. & Wijeratne, P.A. et al. Identifying multiple sclerosis subtypes using unsupervised machine learning and MRI data. *Nat Commun* 12, 2078 (2021). <https://doi.org/10.1038/s41467-021-22265-2>
- [21] Pontillo, G., Penna, S. & Cocozza, S. et al. Stratification of multiple sclerosis patients using unsupervised machine learning: A single-visit MRI-driven approach. *Eur Radiol* 32, 5382–5391 (2022). <https://doi.org/10.1007/s00330-022-08610-z>
- [22] Reháková, Barbora & Kopal, Jakub & Rasova, Kamila & Tintera, Jaroslav & Hlinka, Jaroslav. Open access: The effect of neurorehabilitation on multiple sclerosis—unlocking the resting-state fMRI Data. *Frontiers in Neuroscience* 15, (2021). <https://doi.org/10.3389/fnins.2021.662784>
- [23] Loizoua, C.P., Petroudis, S., Seimenisc, I., Pantziarisd, M. & Pattichisb, C.S. Quantitative texture analysis of brain white matter lesions derived from T 2-weighted MR images in MS patients with clinically isolated syndrome. (2014). <https://doi.org/10.1016/j.neurad.2014.05.006>
- [24] Constantinou, K.P., Constantinou, I.P., Pattichis, C.S. & Pattichis, M.S. Medical image analysis using AM-FM models and methods. in *IEEE Reviews in Biomedical Engineering*, 14, 270–289 (2021). <https://doi.org/10.1109/RBME.2020.2967273>
- [25] Carass, A., Roy, S. & Jog, A. Longitudinal multiple sclerosis lesion segmentation: Resource and challenge. *Neuroimage* 148, 77–102 (2017). <https://smart-stats-tools.org/lesion-challenge-2015>
- [26] Longitudinal multiple sclerosis lesion segmentation challenge. <https://smart-stats-tools.org/lesion-challenge-2015>
- [27] Hu, C., Kang, G., Hou, B., Ma, Y., Labeau, F. & Su, Z. Acu-Net: a 3D attention context UNet for multiple sclerosis lesion segmentation, in: *IEEE International Conference on Acoustics, Speech and Signal Processing (ICASSP 2020)* 1384–1388 (2020). <https://doi.org/10.1109/ICASSP40776.2020.9054616>
- [28] T M, G., Minavathi, & M S, D. Semantic segmentation of kidney tumors using variants of U-Net architecture. *International Journal of Online and Biomedical Engineering (iJOE)*, 18(10), 143–153 (2022). <https://doi.org/10.3991/ijoe.v18i10.31347>
- [29] Y., S. L., Katapally, M., Pabba, K. & Mudunuri, V. Efficient tumor detection in MRI brain images. *International Journal of Online and Biomedical Engineering (iJOE)* 16(13), 122–131 (2020). <https://doi.org/10.3991/ijoe.v16i13.18613>

- [30] Richa, Kaur, K. & Singh, P. A novel MRI and CT image fusion based on discrete wavelet transform and principal component analysis for enhanced clinical diagnosis. *International Journal of Online and Biomedical Engineering (iJOE)* 18(10), 64–82 (2022). <https://doi.org/10.3991/ijoe.v18i10.31969>
- [31] Swetha, M.D., & Aditya, C.R. Sparse feature aware noise removal technique for brain multiple sclerosis lesions using magnetic resonance imaging. *International Journal of Advanced Computer Science and Applications* 13, (2022). <https://doi.org/10.14569/IJACSA.2022.0130664>
- [32] Shivanandappa, Manjunath & Patil, Malini. Efficient resampling features and convolution neural network model for image forgery detection. *Indonesian Journal of Electrical Engineering and Computer Science* 25, 183 (2022). <https://doi.org/10.11591/ijeecs.v25.i1.pp183-190>
- [33] Shivanandappa, Manjunath & Patil, Malini. Extraction of image resampling using correlation aware convolution neural networks for image tampering detection. *International Journal of Electrical and Computer Engineering* 12, 3033 (2022). <https://doi.org/10.11591/ijece.v12i3.pp3033-3043>

## 7 Authors

**Swetha M D** working as an Assistant Professor in Department of Information Science and Engineering at B.M.S. College of Engineering, Bengaluru (email: [shwetha9918@gmail.com](mailto:shwetha9918@gmail.com)).

**Aditya C R** working as an Associate Professor in Department of Computer Science and Engineering at Vidyavardhaka College of Engineering, Mysuru. (email: [adityacr@vce.ac.in](mailto:adityacr@vce.ac.in)).

Article submitted 2022-07-27. Resubmitted 2022-09-08. Final acceptance 2022-09-08. Final version published as submitted by the authors.